

Available online at [www.sciencedirect.com](http://www.sciencedirect.com)**SciVerse ScienceDirect**

Journal of Hydro-environment Research xx (2012) 1–8

---



---

 Journal of  
**Hydro-environment  
 Research**


---



---

[www.elsevier.com/locate/jher](http://www.elsevier.com/locate/jher)

# Numerical prediction of morphological change of straight trapezoidal open-channel

Sung-Uk Choi <sup>a,\*</sup>, Younghoon Joung <sup>b</sup><sup>a</sup> Department of Civil & Environmental Engineering, Yonsei University, Shinchon-dong, Seodaemun-gu, Seoul 120-749, Republic of Korea<sup>b</sup> ISAN Research Institute, ISAN Corporation, Gwanyang-dong, Dongan-gu, Gyeonggi-do 431-060, Republic of Korea

Received 8 March 2011; revised 17 October 2011; accepted 24 November 2011

---

## Abstract

This paper presents a numerical model that is capable of simulating the morphological process of the trapezoidal open-channel. The fact that particles on the sloped side bank do not move in the same direction as the flow adds the difficulty in modeling. The lateral distribution model, which distributes the unit discharge over the width, is used for the flow analysis. Vectorial bedload formula by Kovacs and Parker (1994) is used and channel topography is calculated by solving Exner's equation with the help of sliding algorithm proposed by Menendez et al. (2008). Values of roughness coefficient and lateral eddy viscosity are calibrated using laboratory data sets. Finally, the proposed model is applied to laboratory experiments of Ikeda (1981) and Izumi et al. (1991). Time evolutions of channel cross section and dimensionless shear stress are provided and discussed.

© 2012 International Association for Hydro-environment Engineering and Research, Asia Pacific Division. Published by Elsevier B.V. All rights reserved.

*Keywords:* Morphological process; Sediment transport; Trapezoidal channel; Open-channel flow; Shields stress

---

## 1. Introduction

Alluvial streams are dynamic in nature, changing continuously their shape. Mathematically they constitute a free boundary problem, in which variables should be sought together with the boundary of the problem domain. In a stream, the shape of the channel section is determined by flow condition, sediment properties including the size and its distribution, sinuosity, and etc. For example, Ikeda et al. (1988) showed that increasing gradation in bed materials deepens and narrows the stream. However, if one assumes that the stream is straight and built with uniform sediment, then sediment erosion and deposition, which are functions of flow, change the shape of the stream.

Studies on the shape of stream cross section for a given flow and particle size began in the 1950s. Glover and Florey

(1951) proposed the cross section of the stable channel, given by a cosine function, in which sediment particles on the boundary are under the threshold condition. Conceptually, this channel at the static equilibrium does not transport bedload. However, later, the static equilibrium concept was shown to be invalid for laboratory channels (Wolman and Brush, 1961) and to yield much smaller width of gravel rivers than observed (Ikeda and Izumi, 1990). The other conceptual theory is the dynamic equilibrium. Under this condition, the bedload is actively transported downstream at the channel center without bank erosion. This situation seems to be physically unreasonable because active bedload in the central region implies continuous erosion of the bank due to the gravity. Parker (1978) termed this incompatibility "stable channel paradox," and he first resolved this paradox using the lateral momentum transfer due to turbulence.

Sediment particles placed on a flat bed initiate their motions if a certain mechanistic condition is met. In this case, the direction of particle movement is the same as that of the flow.

---

\* Corresponding author.

E-mail addresses: [schoi@yonsei.ac.kr](mailto:schoi@yonsei.ac.kr) (S.-U. Choi), [truss96@yonsei.ac.kr](mailto:truss96@yonsei.ac.kr) (Y. Joung).

However, if particles are placed on a bank inclined laterally, the direction of the sediment transport does not coincide with the flow direction. This is because of the pull by the gravity in the lateral direction due to the bank slope as well as in the stream-wise direction. Thus, a key issue in predicting the channel cross section of alluvial streams is to assess the particle movement using the vectorial formulation of the transport.

The purpose of the present study is to present a numerical model that is capable of predicting the morphological process of straight, trapezoidal channel whose sides and bottom are covered with uniform sediment. The numerical model consists of three parts, namely hydrodynamic, sediment transport, and morphological components. The lateral distribution model is used to compute the unit discharge over the channel width, and Kovacs and Parker's (1994) formula is used to estimate the bedload. Exner's equation is solved to update the channel shape with the help of sliding algorithm proposed by Menendez et al. (2008). Important parameters such as roughness coefficient and eddy viscosity are calibrated. Then, the proposed model is applied to two laboratory experiments.

## 2. Governing equations

A model, capable of predicting the morphological change of an open-channel, should solve equations of the fluid flow, particle movement on the plane, and channel cross section change. Thus, the numerical model consists of hydrodynamic, sediment transport, and morphological components with an algorithm describing the sliding phenomenon of the sloped bank.

### 2.1. Hydrodynamic equation

In the present study, the lateral distribution model introduced by Wark et al. (1990) and Knight and Shiono (1990) is used. The model, based on the force balance between the gravity, bottom friction, and turbulent shear in a channel cross section, yields the depth-averaged velocity over the channel width. The governing equation of the lateral distribution model can be derived by integrating the three-dimensional Reynolds equations with the rigid lid assumption (Chien, 2010) or obtained directly from the shallow water equations (Vionnet et al., 2004).

In a channel cross section, the lateral distribution of the depth-averaged longitudinal velocity  $U$  can be obtained by solving the following flow equation:

$$ghS_x = B_g C_f U^2 - h \frac{\partial}{\partial y} \left( \bar{\epsilon}_y \frac{\partial U}{\partial y} \right) \quad (1)$$

where  $x$  and  $y$  denote the longitudinal and lateral directions, respectively,  $g$  is gravity,  $h$  is the local flow depth,  $S_x$  is the longitudinal bed slope ( $=\tan \alpha$ , here,  $\alpha$  is the angle of inclination of the bed in the  $x$ -direction),  $B_g$  is the geometrical factor ( $=\sqrt{1+S_x^2+S_y^2}$ , here,  $S_y$  is the lateral bed slope),  $C_f$  is the friction coefficient, and  $\bar{\epsilon}_y$  is the  $y$ -component depth-averaged eddy viscosity. With the help of Manning's

formula, the friction coefficient  $C_f$  in Eq. (1) can be expressed by

$$C_f = \frac{gn^2}{h^{1/3}} \quad (2)$$

where  $n$  is the roughness coefficient. The depth-averaged eddy viscosity is estimated by following relationship:

$$\bar{\epsilon}_y = \chi_y U_* h \quad (3)$$

where  $\chi_y$  is the non-dimensional lateral eddy viscosity coefficient and  $U_*$  is the shear velocity. The value of  $\chi_y$  is an indicative of the rate of mixing in the lateral direction. That is, the larger the value of  $\chi_y$ , the faster the mixing over the width. Fischer et al. (1979) proposed  $\chi_y = 0.15$  from collections of laboratory experiment data sets for straight, rectangular channels. Darby (1999) proposed  $\chi_y = 0.16$  from comparisons between simulated and measured stage-discharge curves in rivers in UK.

The free slip condition at the bank is imposed to solve Eq. (1). That is,

$$\left. \frac{\partial U}{\partial y} \right|_{\text{banks}} = 0 \quad (4)$$

The centered finite difference scheme is used to discretize Eq. (1) with the boundary condition, and Newton–Raphson method is used to solve the resulting non-linear algebraic equations.

### 2.2. Sediment transport equations

The critical condition under which particles on the bank and on the bed initiate their motions is given by the following relationship:

$$\vec{F}_D + \vec{W}_g + \vec{F}_C = 0 \quad (5)$$

where  $\vec{F}_D$  is the drag force providing main driving mechanism,  $\vec{W}_g$  is the submerged weight of the particle tangential to the bed plane, and  $\vec{F}_C$  is the dynamic Coulomb resistive force.

In Fig. 1, the coordinate of  $(x, y, z)$  denotes the Cartesian system, where  $(x, y)$  is the horizontal plane. The coordinate system by the non-orthonormal vectors  $(\hat{s}, \hat{p}, \hat{n})$  provides the bed plane, which is inclined by  $\alpha$  in the  $x$ -direction and by  $\omega$  in the  $y$ -direction, respectively, whereas the coordinate system by  $(\hat{s}, \hat{p}, \hat{n})$  in Fig. 1 is orthogonal. Then, in the coordinate of  $(\hat{s}, \hat{p}, \hat{n})$ , each force component is given by

$$\vec{F}_D = \frac{1}{2} \rho c_D \frac{\pi D^2}{4} |\vec{u}_r| \vec{u}_r \quad (6)$$

$$\vec{W}_g = \rho R g \frac{\pi D^3}{6} \vec{k}_t \quad (7)$$

$$\vec{F}_C = -\vec{t}_{vp} \rho R g \frac{\pi D^3}{6} |\vec{k}_n| \mu_C \quad (8)$$

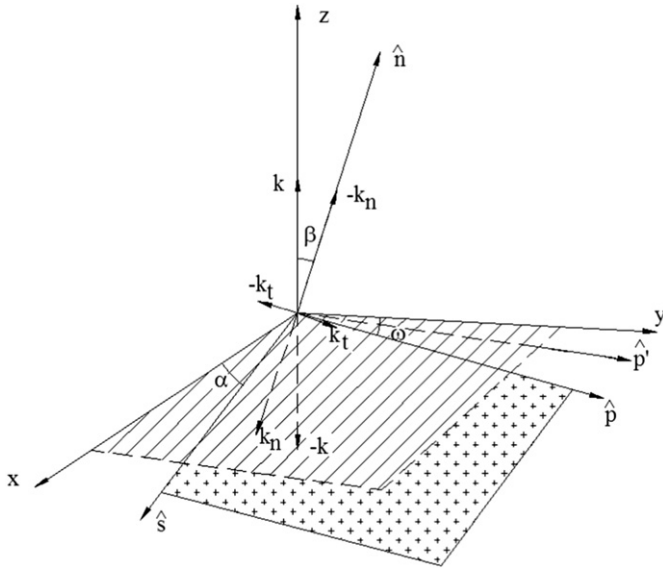


Fig. 1. Coordinate systems used in the sediment transport model in Kovacs and Parker (1994).

where  $\vec{u}_r (= \vec{u}_b - \vec{v}_p)$  is the fluid velocity relative to the moving particle, and  $\vec{k}_n$  and  $\vec{k}_t$  are normal and tangential components of  $\vec{k}$ , respectively, in the bed plane. Using the above expressions, Eqs. (6)–(8), Eq. (5) can be rewritten in the following forms:

$$|\vec{u}_\Delta^*| (u_b^* - v_p^* \cos \psi) - a_c \tau_{c0}^* \left( |\cos \beta| \cos \psi - \frac{\sin \alpha}{\mu_c} \right) = 0 \quad (9)$$

$$|\vec{u}_\Delta^*| v_p^* \sin \psi + a_c \tau_{c0}^* \left( |\cos \beta| \sin \psi - \frac{1}{\mu_c} \frac{\sin \omega \cdot \cos^2 \alpha}{\sqrt{\sin^2 \omega \cdot \cos^2 \alpha + \cos^2 \omega}} \right) = 0 \quad (10)$$

in the  $\hat{s}$  and  $\hat{p}'$  directions, respectively. In Eqs. (9) and (10),  $a_c^{1/2}$  is the conductance factor defined by  $u_b/U_*$  (here,  $u_b$  is the fluid velocity in the bedload layer),  $\mu_c$  is the dynamic Coulomb friction factor,  $\tau_{c0}^*$  is the critical Shields stress for the onset of particle motion on the horizontal bed,  $v_p^*$  is the dimensionless particle velocity ( $= v_p/\sqrt{RgD}$ ),  $u_b^*$  is the dimensionless fluid velocity in the bedload layer ( $= u_b/\sqrt{RgD}$ ), and  $|\vec{u}_\Delta^*| = (u_b^* + v_p^* - 2u_b^*v_p^*\cos\psi)^{1/2}$ . Also,  $\beta$  is the angle between the vertical axis and the normal vector to the bed plane and  $\psi$  is the angle between the direction of particle motion and longitudinal flow direction. In the present study, Newton–Raphson method is used to obtain two unknown variables,  $v_p^*$  and  $\psi$ , in Eqs. (9) and (10) with values of parameters such as  $a_c^{1/2} = 11.9$ ,  $\mu_c = 0.84$ , and  $\tau_{c0}^* = 0.035$  from Kovacs and Parker (1994).

To evaluate the volume rate of bedload transport per unit width, the vectorial formulation proposed by Kovacs and Parker (1994) is used. Menendez et al. (2008) referred to this formula as a mechanistic model because empirical contents are only present at the force parameterization level. Kovacs and Parker's (1994) formula takes the following form:

$$\vec{q}_b = \xi^* \vec{v}_p \quad (11)$$

If one denotes  $q_b^*$  by normalizing  $q_{b\rightarrow}$  by  $\sqrt{RgDD}$ , the longitudinal and lateral components of  $q_b^*$  are respectively given by

$$q_{bx}^* = \xi^* v_p^* \cos \psi \cos \alpha \quad (12)$$

$$q_{by}^* = \xi^* v_p^* \cos \omega \left( \cos \psi \cdot \sin \alpha \cdot \sin \omega + \sin \psi \sqrt{\sin^2 \omega \cdot \cos^2 \alpha + \cos^2 \omega} \right) \quad (13)$$

where  $\xi^*$  is the dimensionless volume of bedload and can be calculated by

$$\xi^* = \frac{\tau_b^* - \tau_B^*}{\mu_c |\cos \beta| \cos \psi - \sin \alpha} \quad (14)$$

in which  $\tau_b^*$  and  $\tau_B^*$  are the dimensionless fluid shear stress acting at the top and bottom of the bedload layer, respectively.

### 2.3. Morphological equation

The morphological change of the channel cross section is accounted for by solving the following Exner's equation:

$$\frac{\partial z_b}{\partial t} + \frac{1}{1 - \lambda_p} \left( \frac{\partial q_{by}}{\partial y} + \frac{\partial q_{bx}}{\partial x} \right) = 0 \quad (15)$$

where  $t$  is the time,  $z_b$  is the bed elevation,  $\lambda_p$  the porosity of the bottom sediment particles, and  $q_{bx}$  and  $q_{by}$  are bedload vectors in  $x$ - and  $y$ -directions, respectively. The assumption of uniformity in the longitudinal direction simplifies Eq. (15) by ignoring  $\partial q_{bx}/\partial x$ . The centered finite difference scheme is used for the numerical solution of Exner's equation.

In the present study, the sliding algorithm proposed by Menendez et al. (2008) is used. That is, at each time step, the lateral slope between two nodes is calculated. If the computed local slope is steeper than the angle of repose, the upper node is lowered so that the slope angle becomes the angle of repose. Then, the height of lower node is increased in order to satisfy the mass conservation of sediment. If the node next to the bank is lowered, then the height of the bank should be lowered and a new node is added at the same height as the previous bank. The slope of this new node in the dry part of the bank is assumed to be the same as the angle of repose. At each time

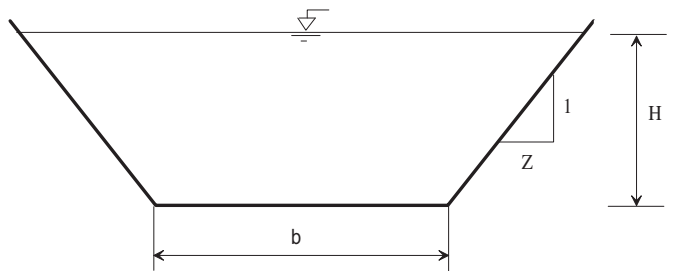


Fig. 2. Schematic sketch of a trapezoidal channel.

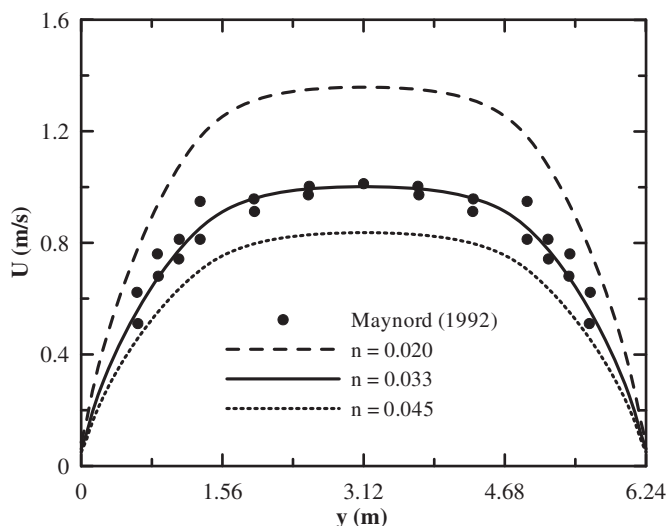


Fig. 3. Impact of roughness coefficient on the depth-averaged velocity.

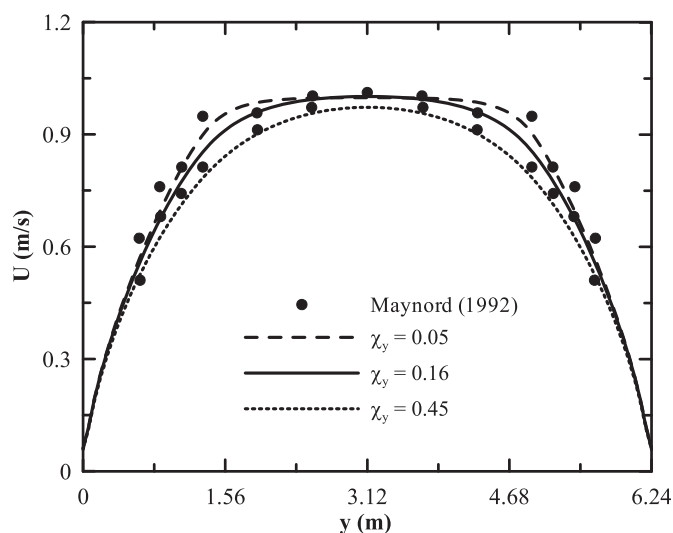


Fig. 4. Impact of non-dimensional eddy viscosity on the depth-averaged velocity.

step, this procedure is repeated until no slope angle larger than the angle of repose is found.

### 3. Parameter study

The flow model is applied to Maynard's (1992) open-channel flow experiment. In the experiment, a trapezoidal channel, whose bottom width ( $b$ ) and the cotangent of the side slope ( $Z$ ) 3.62 m and 2.0, respectively, conveys a discharge of  $2.86 \text{ m}^3/\text{s}$  (see Fig. 2). The longitudinal slope of the channel is 0.002 and

the flow depth is 0.655 m. The depth-averaged velocity profile from the experiment is given by symbols in Fig. 2 while actual data reported in Maynard (1992) are point measurements.

Fig. 3 shows the sensitivity of the roughness coefficient to the lateral distribution of the depth-averaged velocity  $U$ . Respective flow depths are 0.489 m, 0.655 m, and 0.790 m for  $n = 0.020$ , 0.033, and 0.045. The best fit to the data is obtained when  $n = 0.033$ , which is very close to the value of  $n = 0.036$  reported in Maynard (1992). It can be seen that reduction of the roughness coefficient results in the increase in the velocity at the center of the channel and higher velocity gradient near the sidewall.

Fig. 4 depicts the sensitivity of the non-dimensional eddy viscosity to the lateral distribution of the depth-averaged velocity  $U$ . Here, the variation of flow depth depending on eddy viscosity is ignored. The best fit to the data is obtained when  $\chi_y = 0.16$  is used. This value of the non-dimensional eddy viscosity is identical to that obtained by Darby (1999).

The gravity and bottom friction terms in Eq. (1) change rapidly at the interface between the bottom and side slopes, which creates the shear layer there due to the velocity difference. Eddy viscosity plays a role of reducing the velocity difference. Thus, the higher values of eddy viscosity make the velocity distribution smoother, as noted in the figure.

### 4. Applications and results

The proposed model is first applied to a dataset RUN 17 of Ikeda's (1981) experiments. Ikeda (1981) observed a morphological process resulting from erosion of the bank in a flume that is 15 m long and 0.5 m wide. He built a trapezoidal channel with well-graded sands whose mean diameter is 1.3 mm. Detailed flow conditions are given in Table 1.

Fig. 5 shows simulated profiles of the channel cross section at different times. For comparisons, both measured data of Ikeda (1981) and simulated results by Kovacs and Parker (1994) are given. It can be seen that the proposed numerical model predicts well the overall morphological process. At  $t = 1$  h, however, more erosion in the upslope part of the bank is noticed, resulting less deposition on the downslope part of the bank and channel bottom. A similar trend is also observed in the computed profile by Kovacs and Parker (1994). At  $t = 4$  and 12 h, the proposed model predicts the widening of the channel better than the model by Kovacs and Parker (1994) when compared with measured data. The time of  $t = 12$  h corresponds to the termination of experiments by Ikeda (1981). At this time, the channel center becomes nearly flat, suggesting significant decrease in the non-dimensional shear stress, as will be shown later. According to simulated profiles, the front of erosion is located at  $y = 0.07, 0.08, 0.06$ , and

Table 1  
Flow conditions in each laboratory experiments.

	$H$ (m)	$b$ (m)	$Z$	$Q$ ( $\text{m}^3/\text{s}$ )	$U$ (m/s)	$S_x$	$Re$	$D_m$ (mm)	s.g.
Ikeda (1981)	0.061	0.220	1.8	0.004	0.2	0.0021	12,200	1.3	2.65
Izumi et al. (1991)	0.0276	0.20	0.6	0.00082	0.12	0.0024	3300	2.6	1.406

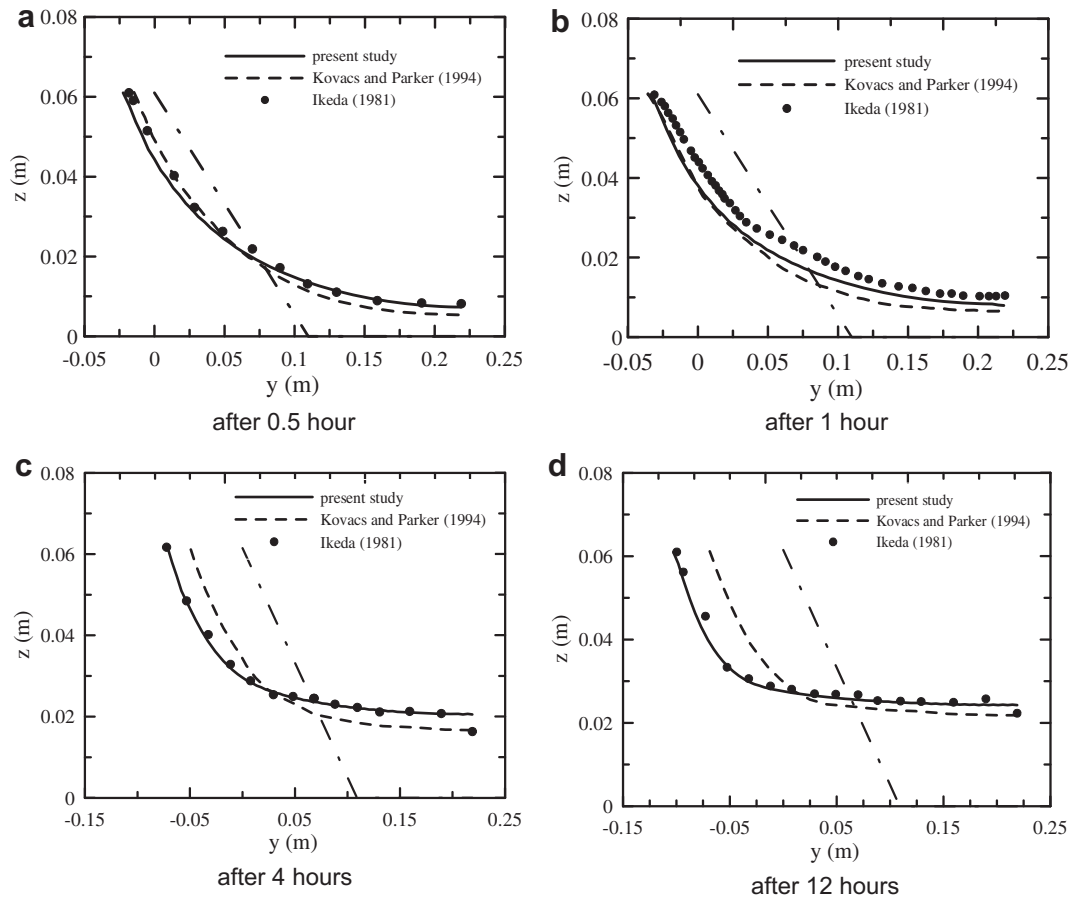


Fig. 5. Change of channel cross section with time.

0.06 m at  $t = 0.5, 1.0, 4.0,$  and  $12.0$  h, respectively. This indicates that the front moves upslope, as described by Kovacs and Parker (1994).

Fig. 6 shows the change of the top width and flow depth at the channel center with time. The width and flow depth are normalized by their initial values. It can be seen that both change rapidly at the initial stage, say up to 3 h, then they change pretty linearly with time. The figure shows that the proposed numerical model predicts the change of width and flow depth better than Kovacs and Parker's model.

Fig. 7 shows the time change of non-dimensional stress at the channel center. The simulated profile indicates a rapid drop of the shear stress at the initial stage, then it shows a gradual decay. The simulated non-dimensional shear stress at the beginning is about 1.7 and becomes 1.05 after 12 h. Together with Fig. 4(d), the figure suggests that, at  $t = 12$  h, the channel reaches nearly the dynamic equilibrium with a small amount of bedload at the channel center without further widening of the side bank. When compared with Kovacs and Parker's (1994) result, the proposed model shows more rapid drop of the non-dimensional shear stress at the early stage. The non-dimensional shear stress by Kovacs and Parker (1994) is about 1.35 after 12 h, which is larger than that from present model. This is due to the less fast widening of the channel simulated by Kovacs and Parker (1994).

The next application is to Izumi et al.'s (1991) experiments. The experiments were performed at St. Anthony Falls Laboratory in University of Minnesota with a 13 m long and 0.6 m wide channel. They used crushed walnut shells, whose specific gravity is 1.046, to increase mobility of sediment particles.

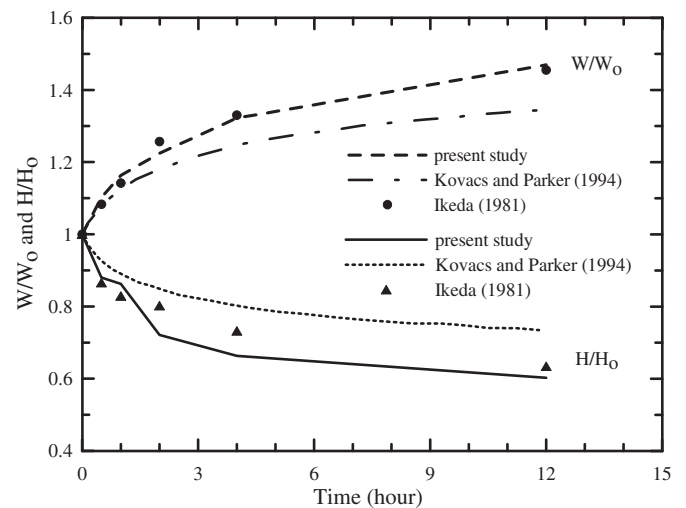


Fig. 6. Change of water surface width and flow depth at the center of the channel (Ikeda's Exp).

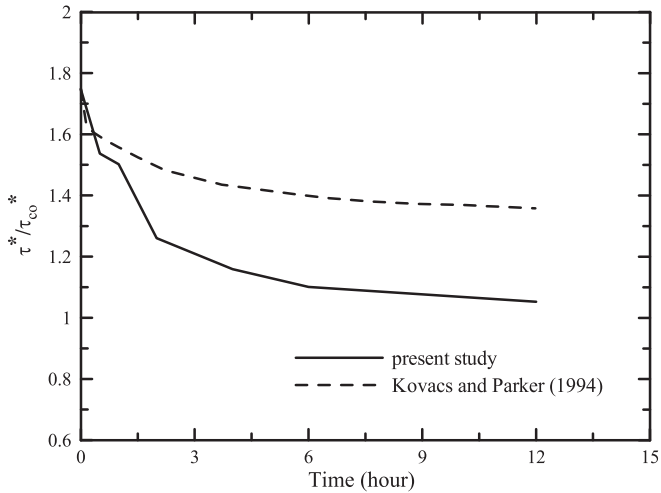


Fig. 7. Change of non-dimensional shear stress at the channel center with time.

This enabled Izumi et al. not to generate such high Reynolds number flows as in Ikeda's (1981) experiment. Detailed flow conditions are provided in Table 1.

Fig. 8 shows the evolution of the channel cross section with time. It can be seen that the model reproduces successfully the widening of the sidewall and sediment deposition on the channel bed of the trapezoidal channel. Similarly to the previous application, erosion of the upper part of the bank takes place, and the eroded sediment particles are deposited on

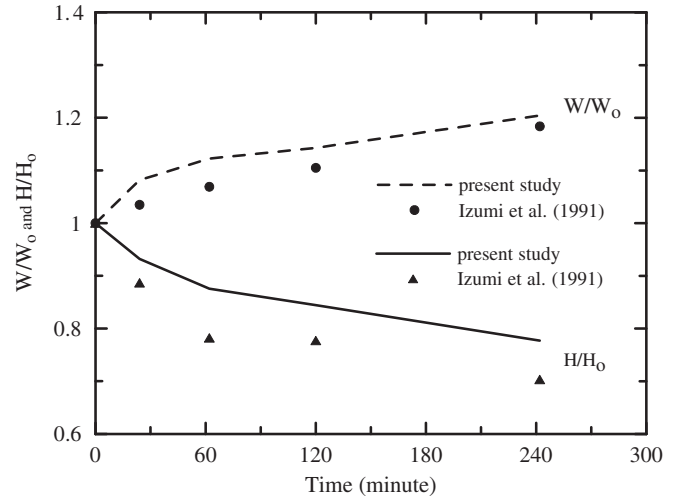


Fig. 9. Change of water surface width and flow depth at the center of the channel (Izumi et al.'s Exp).

the channel bed. Simulated results indicate that the traces of the front of erosion are  $y = 0.051, 0.048, 0.047,$  and  $0.045$  at  $t = 24, 62, 120,$  and  $242$  min, respectively. Like the previous application, this suggests that the front of erosion moves upslope, reaching the dynamic equilibrium.

Fig. 9 shows the time variation of the normalized top width and flow depth at the channel center. It appears that the present

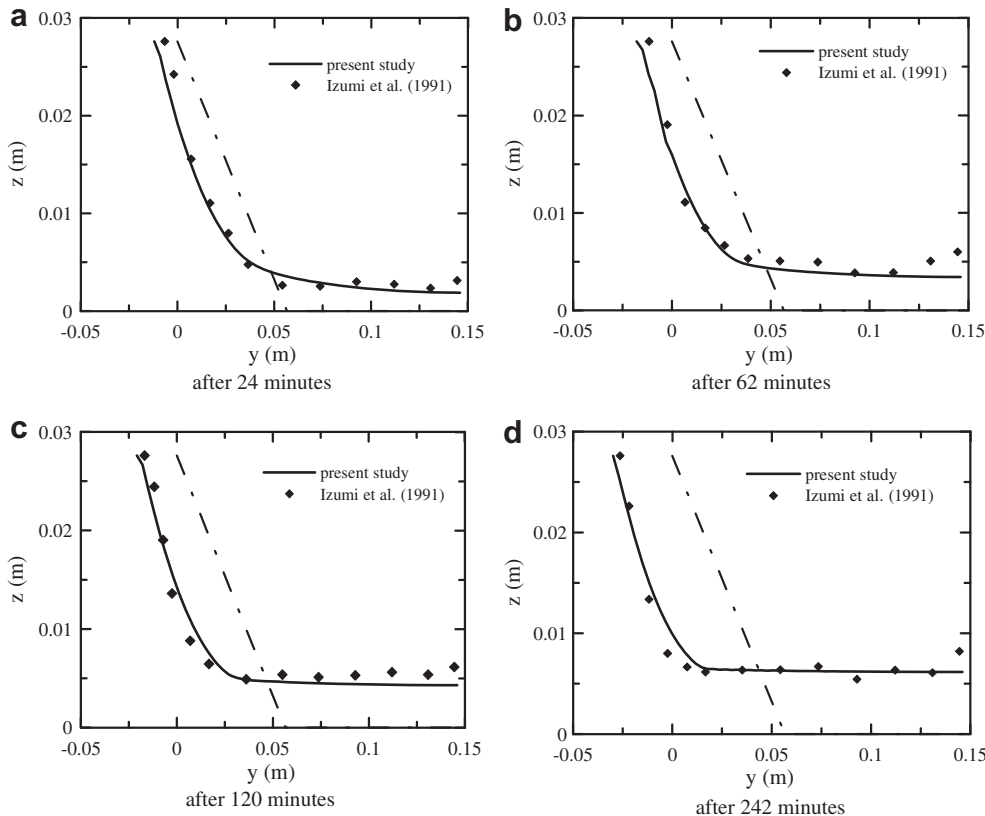


Fig. 8. Change of channel cross section with time.

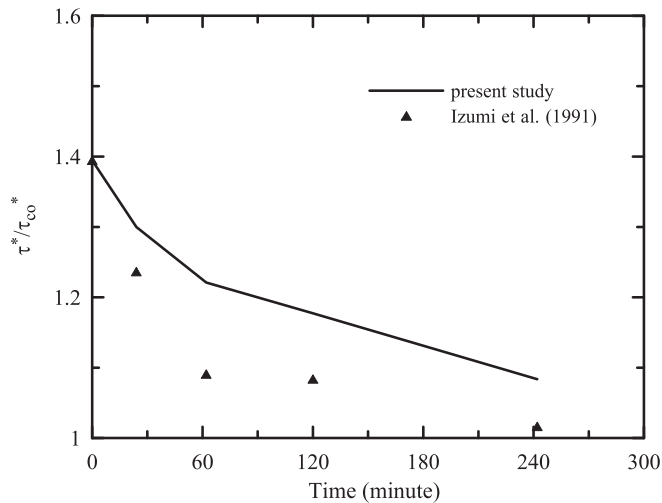


Fig. 10. Change of non-dimensional shear stress at the channel center with time.

model slightly over-predicts the top width, but significantly the flow depth. The over-prediction of the flow depth is due to unexpected deposition at the channel center measured in the experiments. In fact, *Izumi et al. (1991)* used a half-channel, where a vertical steel wall served as the channel center. The trend of changing the width and flow depth is similar to that observed in the application to *Ikeda (1981)*.

Fig. 10 shows the time change of the non-dimensional shear stress at the channel center. Both simulated and measured data indicate a rapid drop of the shear stress at the initial time, say up to 60 min, then they change gradually. The change of measured shear stress appears to be steeper than simulated result. The non-dimensional shear stress at the beginning is 1.4, and the simulated value after  $t = 240$  min is about 1.1, larger than the observed of 1.02.

## 5. Conclusions

The present paper introduced a numerical model that is capable of simulating the morphological change of a straight, trapezoidal open-channel. The computational procedures take three steps, namely flow prediction, estimation of bedload transport, and building the new channel shape in response to the bedload transport.

The lateral distribution model is used for flow prediction, and the vectorial formula proposed by *Kovacs and Parker (1994)* was used for the estimation of bedload transport. Exner's equation was solved to update the channel shape with the help of the sliding algorithm by *Menendez et al. (2008)*.

Regarding the roughness coefficient and non-dimensional eddy viscosity, a parameter study was performed by applying the flow model to laboratory experiments of the trapezoidal channel flow. The model successfully reproduces the lateral distribution of the unit discharge with values of  $n = 0.033$  and  $\chi_y = 0.16$ . The former is very close to the value reported through experiments and the latter is identical to the value proposed by *Darby (1999)*. The flow model is found to

be more sensitive to the roughness coefficient than to the non-dimensional eddy viscosity.

Then, the model was applied to *Ikeda's (1981)* and *Izumi et al.'s (1991)* experiments for the morphological change of the trapezoidal channel section. Both experiments use similar channel dimensions and flow conditions, but *Izumi et al.* used light sediment particles to facilitate the morphological change. It was shown that the proposed model successfully predicts the morphological process with time, i.e., widening of the sidewall and deposition on the lower part of the sidewall and channel bed. The widening of the sidewall and sediment deposition at the channel center occur rapidly at the initial stage, then they slowed down. As it gets close to the equilibrium, the channel bed became flattened due to sediment deposition, characterized by non-dimensional shear stress slightly larger than unity. This corresponds to the dynamic equilibrium termed by *Parker (1978)* under which condition widening of the sidewall ceases with a little bedload at the channel center.

## Acknowledgments

This work was supported by a grant (Code # '11 CTIP C-04) from the Construction Technology Innovation Program (CTIP) funded by from the Ministry of Land, Transport and Maritime Affairs of Korean government.

## References

- Chien, C.V., 2010. Prediction of morphological change of straight open-channel. Master's thesis, Yonsei University, Seoul, Korea.
- Darby, S.E., 1999. Effect of riparian vegetation on flow resistance and flood potential. *Journal of Hydraulic Engineering*, ASCE 129 (6), 474–478.
- Fischer, H.B., List, E.J., Koh, R.C.Y., Imberger, J., Brooks, N.H., 1979. *Mixing in Inland and Coastal Waters*. Academic Press, San Diego, CA.
- Glover, R.E., Florey, Q.L., 1951. *Stable Channel Profiles*. Hydraulics Laboratory Report 325. Hydraulics Laboratory, US Bureau of Reclamation, Washington, DC.
- Ikeda, S., 1981. Self-formed straight channels in sandy beds. *Journal of the Hydraulics Division*, ASCE 107 (HY4), 389–406.
- Ikeda, S., Izumi, N., 1990. Width and depth of self-formed straight gravel rivers with bank vegetation. *Water Resources Research*, AGU 26 (10), 2353–2364.
- Ikeda, S., Parker, G., Kimura, Y., 1988. Stable width and depth of straight gravel rivers with heterogeneous bed materials. *Water Resources Research*, AGU 24 (5), 713–722.
- Izumi, N., Kovacs, A., Parker, G., Leuthe, D.P., 1991. *Experimental and Theoretical Studies of Bank Erosion in Rivers and its Prevention by Low-cost Means*. Saint Anthony Falls Hydraulic Laboratory Project Report No. 320.
- Knight, D.W., Shiono, K., 1990. Turbulence measurements in a shear layer region of a compound channel. *Journal of Hydraulic Research*, IAHR 18 (2), 175–196.
- Kovacs, A., Parker, G., 1994. A new vector bed load formulation and its application to the time evolution of straight river channels. *Journal of Fluid Mechanics* 267, 153–183.
- Maynard, S.T., 1992. *Riprap Stability: Studies in Near-Prototype Size Laboratory Channel*. Technical Report No. HL-92-5. U.S. Corps of Engineers, Waterways Experiment Station, Vicksburg, MS.
- Menendez, A.N., Laciana, C.E., Garcia, P.E., 2008. An integrated hydrodynamic–sedimentologic–morphologic model for the evolution of alluvial channels cross sections. *Engineering Applications of Computational Fluid Mechanics* 2 (4), 411–426.

- Parker, G., 1978. Self-formed straight rivers with equilibrium banks and mobile bed. Part 2. The gravel river. *Journal of Fluid Mechanics* 89, 127–146.
- Vionnet, C.A., Tassi, P.A., Martin Vide, J.P., 2004. Estimates of flow resistance and eddy viscosity coefficients for 2D modeling on vegetated floodplains. *Hydrological Processes* 18, 2907–2926.
- Wark, J.B., Samuels, P.G., Ervine, D.A., 1990. A practical method of estimating velocity and discharge in a compound channel. In: White, W.R. (Ed.), *River Flood Hydraulics*. John Wiley & Sons, Inc., Chichester, UK, pp. 163–172.
- Wolman, M.G., Brush, L.M., 1961. Factors Controlling the Size and Shape of Stream Channels in Coarse, Non-cohesive Sands. Professional Paper No. 282-G. US Geological Survey.